2013 Project Report

The role of pore-fluid pressure on fault behavior at the base of the seismogenic zone

Greg Hirth and Nick Beeler

Summary: To characterize stress and deformation style at the base of the seismogenic zone we developed a conceptual model and investigated how the mechanical properties of fluid-rock systems respond to variations in temperature and strain rate. The role of fluids on the processes responsible for the brittle-ductile transition in quartz-rich rocks has not been explored at experimental conditions where the kinetic competition between microcracking and viscous flow is similar to that expected in the Earth. Our initial analysis of this competition suggests that the effective pressure law for sliding friction should not work as efficiently near the brittle-ductile transition (BDT) as it does at shallow conditions (*Hirth and Beeler*, 2014; *Beeler et al.*, 2015). Our experiments demonstrate a temperature and strain rate dependence of deformation during semi-brittle flow of quartzite. The resulting "flow law" indicates deformation is rate limited by sub-critical crack growth, potentially in response to emission of dislocation at crack tips. Our results also provide a quantification of the role of water on the strength of quartzites in the semi-brittle flow regime

Technical Report

The effect of pore-fluid pressure on mechanical behavior in the frictional regime is described using the relationship:

$$\sigma_{eff=}(\sigma_n - \alpha P_f), \tag{1}$$

where for most applications the constant α is assumed to be unity. However, at high P-T conditions, where creep and crack healing processes are efficient, α may decrease significantly. Owing to the exponential temperature-dependence of thermally activated processes, changes in α may occur with relatively small spatial/temporal variations. In contrast, for rock failure and frictional sliding at low temperature and pressure, $\alpha \approx 1$ is nearly always observed [e.g., *Handin et al.*, 1963; *Morrow and Byerlee*, 1992]. During frictional sliding at low temperature, the real area of surface contact normalized by the nominal area of contact (A_r/A) is very small. *Scholz* (1990) noted that the effective pressure controlling the strength of faults is related to the fractional area along a fault surface that is supported by pressurized pore space relative to the area that is supported by asperity contact across the fault. Where the area of contact is

vanishingly small, a change in pore pressure within the fault acts in nearly exact opposition to the applied fault normal stress, implying:

$$\alpha = 1 - A_r/A \approx 1. \quad (2)$$

Dieterich and Kilgore (1996), hypothesized that A_r/A can be related to the rheological properties of the mineral grains using the relationship:

$$A_r/A = \sigma_n/\sigma_y, \quad (3)$$

where σ_n is the applied normal stress and σ_y is the yield stress at the frictional contacts, which is controlled by the indentation hardness at low temperature. However, at higher temperatures, σ_y decreases as viscous creep becomes more efficient, leading to an increase in A_r/A (e.g., *Boettcher et al.*, 2007) and potentially a concomitant decrease in α.

To include temperature dependent creep in the effective pressure law for friction, we make two modifications to Eq. (3). First, because *Dieterich and Kilgore* (1996) conducted their experiments dry, for fluid present conditions σ_n should be replaced by σ_{eff}, giving:

$$\alpha \approx 1 - \sigma_{eff}/\sigma_y \quad (4)$$

Second, A_r/A cannot exceed unity, thus Eq. (4) is only applicable where $\sigma_y > \sigma_{eff}$.

The solution of (1) and (4) is

$$\sigma_{eff} = \frac{(\sigma_n - P_f)}{1-(P_f/\sigma_y)}, \quad (5)$$

which provides a first order effective pressure law for high temperature rock friction.

APPLICATION

To illustrate the potential influence of α on stress in the Earth, we construct differential stress ($\Delta\sigma$) versus depth profiles using the temperature and strain rate dependent effective pressure law, a constant μ = 0.6 and a constant fluid pressure gradient defined by λ = 0.4. For a strike-slip environment, the differential stress in the frictional regime can be approximated by

$$\sigma_1 - \sigma_3 = \Delta\sigma = F'(\sigma_v - \alpha P_f), \quad (6)$$

where σ_v is the vertical stress resulting from overburden and $F' = 2\mu/(\mu^2+1)^{1/2}$ (e.g., Zoback and Townend, 2001).

The $\Delta\sigma$ predicted by these relationships is shown in Figure 1a assuming $\sigma_n = \sigma_v$. We used a

composite flow law for the asperity yield stress, $\sigma_y = [1/\sigma_{glide} + 1/\sigma_{disl}\,]^{-1}$, which accounts for dislocation glide at low temperature (we used a constant yield stress of 2 GPa in the glide regime, guided by indentation hardness tests on quartz (*Evans*, 1984)) and dislocation creep at higher temperatures (we used the quartzite flow law of *Hirth et al.*, 2001). The resulting yield stress and α (equation 4) are labeled in Figure 1a. At low temperature and pressure, where σ_y is large, and thus A_r/A is small, the predicted friction law follows the strength depth relationship defined by a hydrostatic pore fluid pressure gradient. However, α decreases with increasing temperature (owing to the temperature effect on creep), and the friction law evolves toward that defined by a lithostatic pressure gradient near the BDT.

Alpha also depends on strain rate through the strain rate dependence of σ_y. We assume a strain rate of 10^{-12}/s throughout the model in Figure 1. This choice is based on an active deformation width of ~1km for a plate displacement rate of ~30 mm/yr (~10^{-9}m/s), consistent with the width of major crustal shear zones (e.g., *Burgmann and Dresen*, 2008) and the width of microseismicity along faults in California (e.g., *Powers and Jordan*, 2010).

As illustrated in Figure 1b, the resulting stress depth diagram is consistent with geological constraints for stress in the earth. The stress just below the BDT (e.g., *Behr and Platt*, 2011) is well predicted by the dislocation creep flow law we employed to constrain σ_y. Values of differential stress greater than that predicted for a friction law with hydrostatic pore-fluid pressure have previously been interpreted to result from co-seismic stress increases. In contrast, the temperature-induced decrease in α suggests that such stresses may occur under nominally steady state creep. For reference, relatively high stresses near the BDT have also been determined directly from bore-hole data and microstructural observations of rocks from the KTB hole drill hole (e.g., *Dresen et al.*, 1997).

The basis for our conceptual model was further explored in a follow up paper (*Beeler et al., submitted*, JGR, 2015) – including an analysis of the potential for changes in alpha to explain the remarkable differences in frictional behavior indicated by tidal triggering of LFE's along the San Andreas Fault.

Experimental Results

Triaxial compression experiments were conducted on Fontainbleau sandstone at temperatures to 900°C and effective pressures to 175 MPa under a range of intragranular water availability. Both yield and peak strengths during semibrittle flow and faulting decrease linearly with an increase in intragranular water concentration C_{OH} (as determined from infrared spectroscopy). Microstructural observations and the effects of strain rate, temperature, and C_{OH} on peak strength suggest that stress-corrosion assisted cataclasis is the dominant mechanism of the pre-failure transient flow. The calculated constitutive behavior is consistent with that reported from subcritical cracking in quartz single crystals. Semi-brittle flow exhibits a temperature-dependent stress exponent, which is well fit by an exponential law with an activation enthalpy of 185 to 250 kJ/mol and Peierls stress of 2.5 to 7.5 GPa. We infer that the dislocation activity at crack tips is the rate-controlling process for the stress-corrosion cracking. Results presented at AGU and SCEC meetings.

Outreach: The results of our project are being presented during lectures for classes and during seminars at other labs, universities and meetings.

Publications

Hirth, G., and N.M. Beeler, The role of fluid pressure on frictional behavior at the base of the seismogenic zone, *Geology*, 43, 223-226, doi: 10.1130/G36361.1, 2015.

Beeler, N.M., G. Hirth, A. Thomas, and R. Burgmann, Effective stress, friction and deep crustal faulting, *J. Geophys. Res.*, revision submitted, 2015.

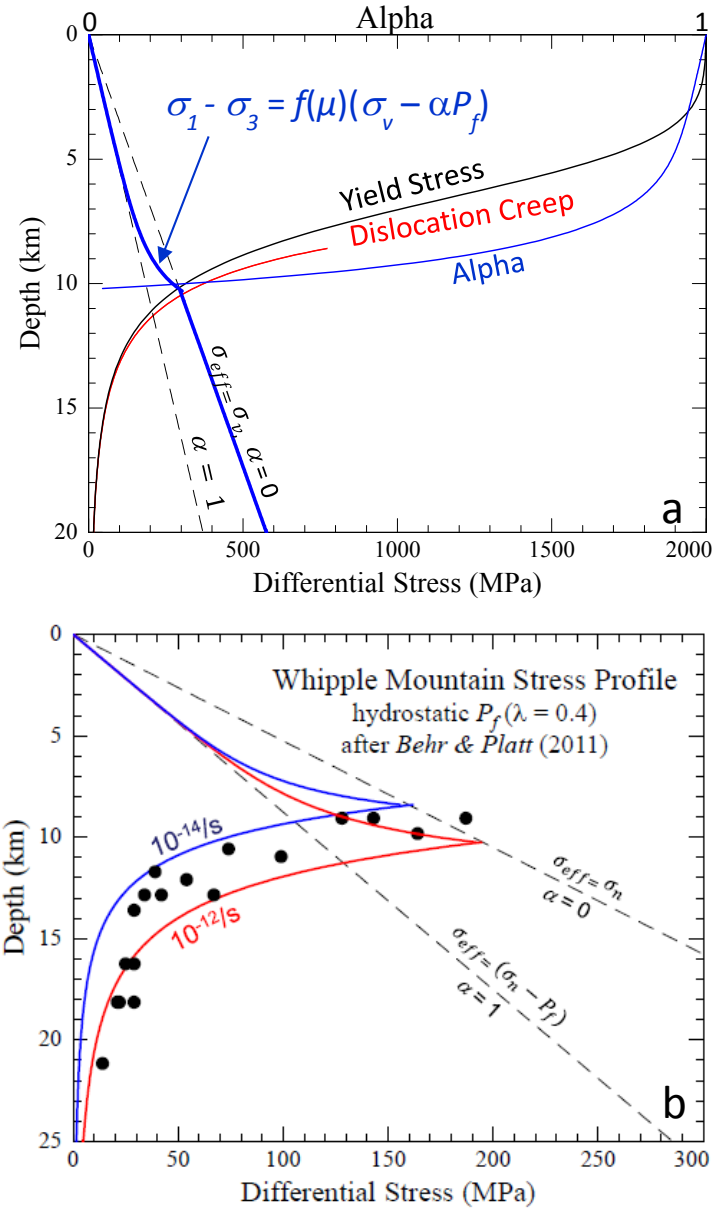

Figure 1: (a) Transition in frictional behavior arising from a decrease in alpha (α) with increasing temperature; frictional stress and the magnitude of alpha (upper x- axis) are shown by blue curves. The yield stress at frictional asperities is shown by the black curve. The yield stress and dislocation creep stress were calculated for a strain rate of 1e-12/s and λ = 0.4. (b) Comparison of stress based on temperature-dependent effective pressure law with estimates based on grain size piezometry of quartz mylonites from the Whipple Detachment (after *Behr and Platt*, 2011). Plot calculated for normal faulting setting with strain rates of 1e-12/s and of 1e-14/s. Dashed lines in both (a) and (b) show frictional stress for an effective normal stress with hydrostatic pore fluid pressure (λ = 0.4 and α = 1) and with a lithostatic normal stress. From *Hirth and Beeler*, 2014.

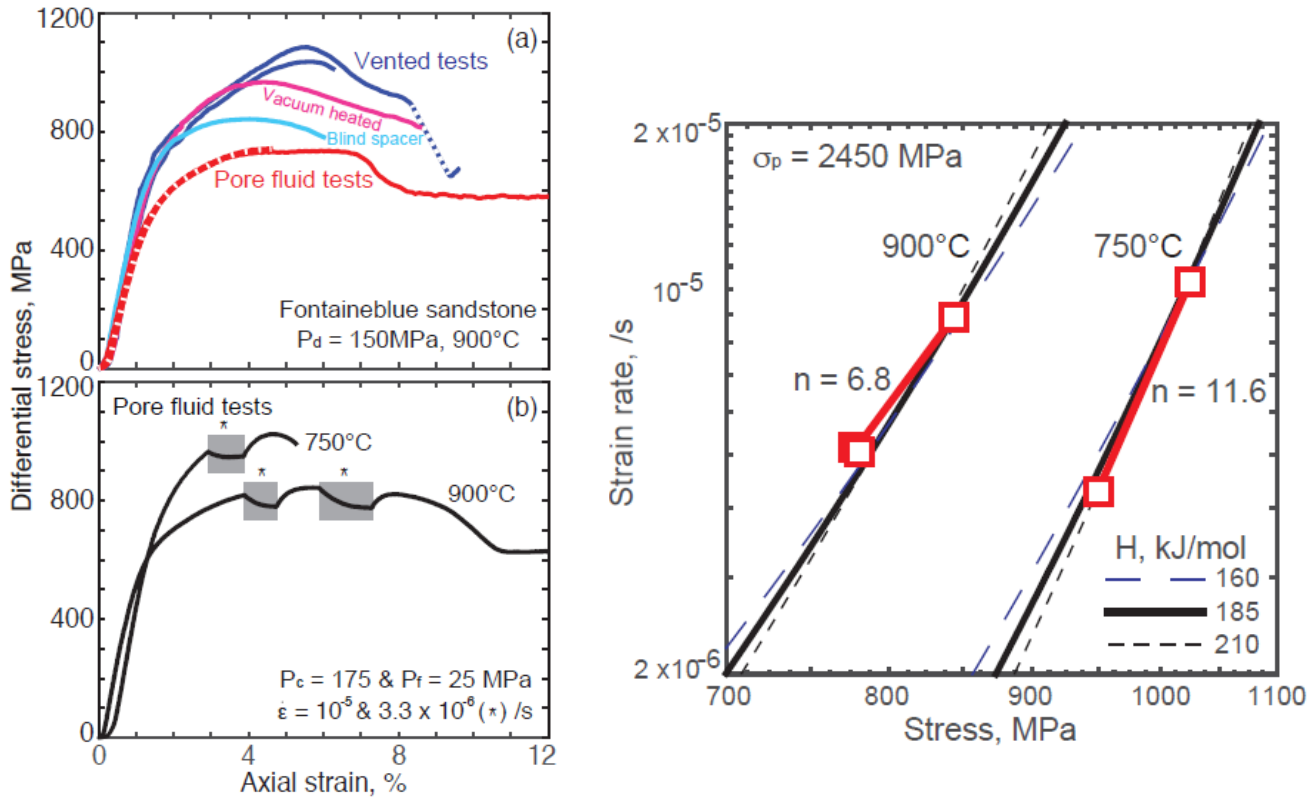

Figure 2. (a) Differential stress vs. axial strain curve plot showing the effect of intra-granular water availability and (b) strain rate on the semi-brittle deformation in Fontainebleau sandstone. Water is lost from samples in vented tests, but remains present in pore-fluid tests in which Argon gas is used as a pore-fluid (P_c = 175, P_f = 25 MPa); vented and blind spacer tests conducted at P_c = 150 MPa. All tests run at $\dot{\varepsilon}_a = 10^{-5}$/s. (b) Results of strain rate stepping tests in pore fluid tests. (c) Log strain rate vs. log differential stress for Fontainebleau sandstone under pore fluid at the temperatures and differential pressures indicated. The stress exponents n from a power law are shown in red; the activation enthalpy (H) for the exponential Peierls law are shown in black.

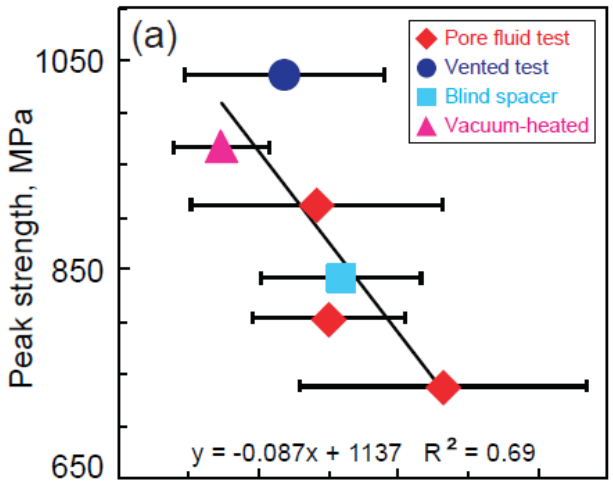

Figure 3. Peak strength and as a function of water concentration. Water contents determined from the median value (solid symbols) and standard deviation (denoted by the error bars) of macroscopic C_{OH} determined by FTIR.

REFERENCES

Behr, W.M., Platt, J.P., 2011, A naturally constrained stress profile through the middle crust in an extensional terrane, Earth and Planetary Science Letters, 303, 181-192.

Boettcher, M., Hirth, G., and Evans, B., 2007, Olivine friction at the base of oceanic seismogenic zones, J. Geophys. Res., 112, B01205, doi:10.1029/2006JB004301

Bürgmann, R. and Dresen, G., 2008, Rheology of the lower crust and upper mantle: evidence from rock mechanics, geodesy, and field observations, An. Rev. Earth Planet. Sci., 36, 531-567, doi: 10.1146/annurev.earth.36.031207.124326.

Dieterich, J.H. and Kilgore, B.D. , 1996, Imaging surface contacts: power law contact distributions and contact stresses in quartz, calcite, glass and acrylic plastic. Tectonophysics, 256, 219–239.

Dresen, G., Duyster, J., Stöckhert, B., Wirth, R., and Zulauf, G., 1997, Quartz dislocation microstructure between 7000 m and 9100 m depth from the Continental Deep Drilling Program KTB, J. Geophys. Res., 102, 18,443-18,452, doi:10.1029/96JB03394.

Evans, B., 1984, The effect of temperature and impurity content on indentation hardness of quartz, J. Geophys. Res., 89, 4213-4222.

Handin, J., Hager, R.V., Friedman, M., and Feathers, J.N., 1963, Experimental deformation of sedimentary rocks under confining pressure: pore pressure tests, Bull. Am. Assoc. Petroleum Geologists, 5, 716-755.

Hirth, G., Teyssier, C., and Dunlap, W.J., 2001, An evaluation of quartzite flow laws based on comparisons between experimentally and naturally deformed rocks, Int. J. Earth Sci., (Geologishe Rundschau), 90, 77-87.

Morrow, C., Radney, B., and Byerlee, J., 1992, Frictional strength and the effective pressure law of montmorillonite and illite clays, in Fault mechanics and transport properties of rocks, ed Evans, Wong, , p 69-88.

Powers, P.M., and Jordan, T.H., 2010, Distribution of seismicity across strike-slip faults in California, J. Geophys. Res., 115, DOI: 10.1029/2008JB006234.

Scholz, C.H., The Mechanics of Earthquakes and Faulting. Cambridge: Cambridge Univ. Press, 1990.